Intraligand Charge Transfer in the Pd(II) Oxinate Complex $Pd(qol)_2$. Site-Selective Emission, Excitation, and Optically Detected Magnetic Resonance

Hartmut Yersin* and Dirk Donges[†]

Institut für Physikalische und Theoretische Chemie, Universität Regensburg, D-93040 Regensburg, Germany

Jeffrey K. Nagle

Department of Chemistry, Bowdoin College, Brunswick, Maine 04011

Rolf Sitters and Max Glasbeek*

Laboratory for Physical Chemistry, University of Amsterdam, Nieuwe Achtergracht 129, 1018 WS Amsterdam, The Netherlands

Received August 24, 1999

The first spectroscopic investigation of $Pd(qol)_2$ ($qol^- = 8$-quinolinolato-*N*,*O* = oxinate) dissolved in an *n*-octane matrix (Shpol'skii matrix) is reported. Application of several spectroscopic methods at liquid helium temperatures (typically, $T = 1.2$ K), such as site-selective and highly resolved luminescence and excitation spectroscopy, time-resolved emission spectroscopy, optically detected magnetic resonance, microwave recovery, phosphorescence microwave double-resonance, and magnetic fields, allows us to characterize the lowest excited electronic states in detail. In accord with previous assignments for the related $Pt(qol)_2$ it is shown that these lowest states represent intraligand charge-transfer states, namely, ^{1}ILCT and ^{3}ILCT. The electronic origin of the ^{1}ILCT state lies at 20 617 cm^{-1} (site A). It exhibits a nearly homogeneous line width with a half-width of about 80 cm^{-1} (fwhm), which corresponds to a lifetime of $\tau(^1\text{ILCT}) \approx 2 \times 10^{-13}$ s. This value is even shorter than that found for $Pt(qol)_2$, presumably due to intersystem crossings and relaxations to dd* states. The electronic origin of the ^{3}ILCT state lies at 16 090 cm^{-1} (site A), and its zero-field splittings (zfs) into three sublevels are $2E = 2356$ MHz (0.0785 cm^{-1}) and $D - E = 5241$ MHz (0.175 cm^{-1}). The emission decay times of the three sublevels are determined as $\tau_{\mathbf{I}} = 90 \pm 30$ ms, $\tau_{\mathbf{II}} = 180 \pm 10$ μs, and $\tau_{\mathbf{III}} = 80 \pm 10$ μs. (Slightly different values are found for a second site B at 16 167 cm^{-1}.) From the small values of zfs and the long emission decay times it is concluded that metal-d or MLCT admixtures to ^{3}ILCT are very small. This result clearly reflects the ligand-centered character of the transition. The assignment as an ILCT transition is supported by the occurrence of relatively strong vibrational satellites of Pd−N and Pd−O character in highly resolved emission spectra. Although the transition is ascribed to a charge-transfer process, the geometry changes between the ground state and ^{3}ILCT are very small. The results found for $Pd(qol)_2$ are compared to those of companion studies of $Pt(qol)_2$ and $Pt(qtl)_2$ ($qtl^- =$ 8-quinolinethiolato-*N*,*S*).

1. Introduction

Transition metal complexes with organic ligands have been investigated with increasing interest due to the large number of potential photocatalytic and photophysical applications. (For instance, see the examples cited in ref 1.) Most of these applications depend on the properties of the lowest excited electronic states and the ground state. In particular, for compounds with open shell metal ions of the platinum metal group the photoactive states are the lowest triplets. This is because, following an excitation into higher lying singlets, these triplets are populated by very fast intersystem crossing processes. Only a small number of research groups have carried out systematic investigations of these triplets by use of powerful methods of laser spectroscopy, to obtain spectrally highly resolved (on the order of 1 cm^{-1}) and time-resolved emission and excitation spectra (e.g., see refs 1−10). For several

* To whom correspondence should be addressed.

[†] Present address: Lambda Physik GmbH, Hans-Boeckler-Strasse 12, D-37079 Göttingen, Germany.

(1) Yersin, H.; Humbs, W.; Strasser, J. In *Electronic and Vibronic Spectra of Transition Metal Complexes, Vol. II*; Yersin, H., Ed.; Topics in Current Chemistry 191; Springer-Verlag: Berlin, 1997; p 153.
(2) Braun, D.; Hensler, G.; Gallhuber, E.; Yersin, H. *J. Phys. Chem.* **1991**, *95*, 1067.
(3) Humbs, W.; Yersin, H. *Inorg. Chem.* **1996**, *35*, 2220.
(4) Yersin, H.; Humbs, W.; Strasser, J. *Coord. Chem. Rev.* **1997**, *159*, 325.
(5) Zilian, A.; Güdel, H. U. *Inorg. Chem.* **1992**, *31*, 830.
(6) Strouse, G. F.; Güdel, H. U., Bertolasi, V.; Ferretti, V. *Inorg. Chem.* **1995**, *34*, 5578.
(7) Colombo, M. G.; Hauser, A.; Güdel, H. U. In *Electronic and Vibronic Spectra of Transition Metal Complexes, Vol. I*; Yersin, H., Ed.; Topics in Current Chemistry 171; Springer-Verlag: Berlin, 1994; p 143.
(8) Chen, W.-H.; Rieckhoff, K. E.; Voigt, E.-M. *Chem. Phys.* **1986**, *102*, 193.
(9) Schmidt, J.; Strasser, J.; Yersin, H. *Inorg. Chem.* **1997**, *36*, 3957.

10.1021/ic991023l CCC: $19.00
Published on Web 02/03/2000

compounds, it was possible to achieve a detailed characterization of properties of the triplet sublevels. In some cases even the dynamical behavior[1,9−15] within the system of these sublevels could be determined. Characterizations of these triplets were particularly successful for compounds with zero-field splittings (zfs) on the order of several cm^{-1}. In this situation, the triplet sublevels may optically be well resolved and thus investigated individually (e.g., see refs 1, 2, 4, 9, and 12−15). However, many interesting complexes exhibit zfs on the order of only 0.1 cm^{-1} (3 GHz), which are not easily optically resolvable. In this situation, optical spectroscopy with additional microwave irradition allows one in favorable cases to enhance the spectral resolution by orders of magnitude into the megahertz range (30 MHz ≙ 0.001 cm^{-1}). The feasibility of this method, in particular of ODMR (optically detected magnetic resonance) spectroscopy (e.g., see ref 16) is well established for transition metal complexes (e.g., see refs 11 and 17−25). From these measurements, detailed information concerning the fine structure parameters (D and E) and the radiative character of the phosphorescent triplet sublevels were obtained. For example, it could be concluded that the emission of Rh(III) chelates is ligand-centered and mainly of $^3\pi\pi^*$ nature.[20−22] (Compare also ref 3.) Very recently, an optical-microwave double resonance study for a metal−organic chelate compound, namely, $Pd(2\text{-thpy})_2$ ($(2\text{-thpy})^- = 2$-thienylpyridinate), in the lowest excited triplet state was reported.[11] This investigation demonstrated, for example, the complementary nature of time-resolved emission spectroscopy[10] and PMDR (phosphorescence microwave double-resonance) spectroscopy. Interestingly, both methods[10,11] can reveal a spin selectivity in the vibrational satellite lines of the emission spectrum.

In the present investigation, we report on results obtained for $Pd(qol)_2$ (structural formula in Figure 2) ($qol^- = 8$-quinolinolato-*N*,*O* = oxinate). This compound is related to the well-known $Al(qol)_3$,[26−29] which plays a crucial role in white-light-emitting organic electroluminescent devices (OLEDs). Such devices may constitute building blocks for next-generation flat panel display systems.[27,28] In a previous investigation,[26] it has been shown that such $M(qol)_n$ compounds with closed shell metal ions predominantly exhibit fluorescence, such as $Al(qol)_3$, while those with open shell metal ions show phosphorescence, as in $Pt(qol)_2$. The corresponding transitions have been assigned to intraligand charge-transfer (ILCT) transitions.[26] To our knowledge, the electronic structure of the lowest excited states of $Pd(qol)_2$ has not yet been studied in detail. Recently, investigations using methods of emission and excitation spectroscopy for the related compounds, $Pt(qol)_2$ and $Pt(qtl)_2$ ($qtl^- = 8$-quinolinethiolato-*N*,*S*)), provided extensive insight into the nature of ILCT transitions.[30−33] In the present work $Pd(qol)_2$ is investigated by means of high-resolution and site-selective emission spectroscopy as well as by methods involving microwave double-resonance spectroscopy to develop a detailed understanding of the properties of the lowest excited states.

2. Experimental Section

$Pd(qol)_2$ was synthesized in a manner similar to that described by Ballardini et al.[26] for $Pt(qol)_2$. (Compare also refs 30 and 34.) Since $Pd(qol)_2$ is not soluble in *n*-alkanes, it was first dissolved in a solvent of intermediate polarity (1,4-dioxane) and subsequently diluted in *n*-octane. The volume ratio of 1,4-dioxane to *n*-octane was about 1:50, yielding a $Pd(qol)_2$ concentration of about 10^{-5} mol/L. After the solution was transferred into a cell of 2 mm inner diameter, it was frozen at a cooling rate of about 100 K/min, thus forming the Shpol'skii matrix. The ODMR spectrometer is described elsewhere.[11,35] The optical excitation for the ODMR experiments was carried out by use of the 457.9 nm line of a cw Ar^+ ion laser. Small magnetic fields (up to ∼400 G) for ODMR measurements were applied by means of superconducting Helmholtz coils immersed in the liquid bath, while for application of high magnetic fields (up to 12 T for emission measurements) an Oxford Instruments superconducting magnet was used (MD 10-S). Temperatures below 4.2 K were achieved by pumping off the helium. Details of the optical setup for recording emission and excitation spectra[3,36] and of the equipment for measurements of emission lifetimes,[9] respectively, are described elsewhere.

3. Results and Discussion

$Pd(qol)_2$ exhibits a planar trans-coordination.[34] (See the inset of Figure 2.) Further, the length of the complex (1.26 nm) fits perfectly to the length of *n*-octane (1.25 nm).[37] Thus, it is expected that *n*-octane represents a suitable Shpol'skii matrix[38] for $Pd(qol)_2$. Indeed, this doping is successful, yielding spectra which are about 300 times better resolved than reported by other research groups for any oxinate complex (e.g., compare ref 26). Therefore, this matrix was used for all measurements in the present investigation.

3.1. Triplet Emission. A nonselective excitation at 457.9 nm (21 839 cm^{-1}) of $Pd(qol)_2$ in *n*-octane shows that two dominant sites emit and that their spectra are superimposed. The low-energy site A with the $T_1 \rightarrow S_0$ origin at 16 090 cm^{-1} carries (at $T = 4.2$ K) about 75% of the total emission intensity, while the high-energy site B with the electronic origin at 16 167 cm^{-1} occurs with an emission intensity of about 25%. By selective

(10) Schmidt, J.; Wiedenhofer, H.; von Zelewsky, A.; Yersin, H. *J. Phys. Chem.* **1995**, *99*, 226.
(11) Glasbeek, M.; Sitters, R.; van Veldhoven, E.; von Zelewsky, A.; Humbs, W.; Yersin, H. *Inorg. Chem.* **1998**, *37*, 5159.
(12) Yersin, H.; Strasser, J. *J. Lumin.* **1997**, *72−74*, 462.
(13) Strasser, J.; Donges, D.; Humbs, W.; Kulikova, M. V.; Balashev, K. P.; Yersin, H. *J. Lumin.* **1998**, *76−77*, 611.
(14) (a) Strasser, J.; Homeier, H. H. H.; Yersin, H. *Chem. Phys.*, submitted for publication. (b) Yersin, H.; Strasser, J. *Coord. Chem. Rev.*, in press.
(15) Homeier, H. H. H.; Strasser, J.; Yersin, H. *Chem. Phys. Lett.* **2000**, *316*, 280.
(16) Clarke, R. H. Ed. *Triplet State ODMR Spectroscopy*, Wiley: New York, 1982.
(17) Komada, Y.; Yamauchi, S.; Hirota, N. *J. Phys. Chem.* **1986**, *90*, 6425.
(18) van Oort, E.; Sitters, R.; Scheijde, J. H.; Glasbeek, M. *J. Chem. Phys.* **1987**, *87*, 2394.
(19) Kamyshny, A. L.; Suisalu, A. P.; Aslanov, L. A. *Coord. Chem. Rev.* **1992**, *117*, 1.
(20) Westra, J.; Glasbeek, M. *Chem. Phys. Lett.* **1990**, *166*, 535.
(21) Giesbergen, C. P. M.; Terletski, C.; Frei, G.; Güdel, H. U.; Glasbeek, M. *Chem. Phys. Lett.* **1993**, *213*, 597.
(22) Giesbergen, C. P. M.; Glasbeek, M. *J. Phys. Chem.* **1993**, *97*, 9942.
(23) Miki, H.; Shimada, M.; Azumi, T.; Brozik, J. A.; Crosby, G. A. *J. Phys. Chem.* **1993**, *97*, 11175.
(24) Miki, H.; Azumi, T. *J. Phys. Chem.* **1994**, *98*, 6059.
(25) Glasbeek, M. In *Transition Metal and Rare Earth Compounds—Excited States, Transitions, Interactions*; Yersin, H., Ed.; Topics in Current Chemistry; Springer-Verlag: Berlin, in press.
(26) Ballardini, R.; Varani, G.; Indelli, M. T.; Scandola, F. *Inorg. Chem.* **1986**, *25*, 3858.
(27) Kido, J.; Kimura, M.; Nagai, K. *Science* **1995**, *267*, 1332.
(28) Salbeck, J. *Ber. Bunsen-Ges. Phys. Chem.* **1996**, *100*, 1667.
(29) Humbs, W.; van Veldhoven, E.; Zhang, H.; Glasbeek, M. *Chem. Phys. Lett.* **1999**, *304*, 10.
(30) Donges, D.; Nagle, J. K.; Yersin, H. *Inorg. Chem.* **1997**, *36*, 3040.
(31) Donges, D.; Nagle, J. K.; Yersin, H. *J. Lumin.* **1997**, *72−74*, 658.
(32) Donges, D. Ph.D. Thesis, Universität Regensburg, 1997.
(33) Vogler, A.; Kunkely, H. *Inorg. Chim. Acta* **1981**, *54*, L273.
(34) Prout, C. K.; Wheeler, A. G. *J. Chem. Soc. A* **1966**, 1286.
(35) Glasbeek, M.; Hond, R. *Phys. Rev. B* **1981**, *23*, 4220.
(36) (a) Yersin, H.; Gliemann, G. *Messtechnik (Braunschweig)* **1972**, *80*, 99. (b) Stock, M.; Yersin, H. *Chem. Phys. Lett.* **1976**, *40*, 423.
(37) Nakhimovsky, L. A.; Lamotte, M.; Joussot-Dubien, J. *Handbook of Low-Temperature Electronic Spectra of Polycyclic Aromatic Hydrocarbons*; Elsevier Science Publishers: Amsterdam, 1989.
(38) Shpol'skii, E. V. *Sov. Phys. Usp. (Engl. Transl.)* **1960**, *3*, 372.

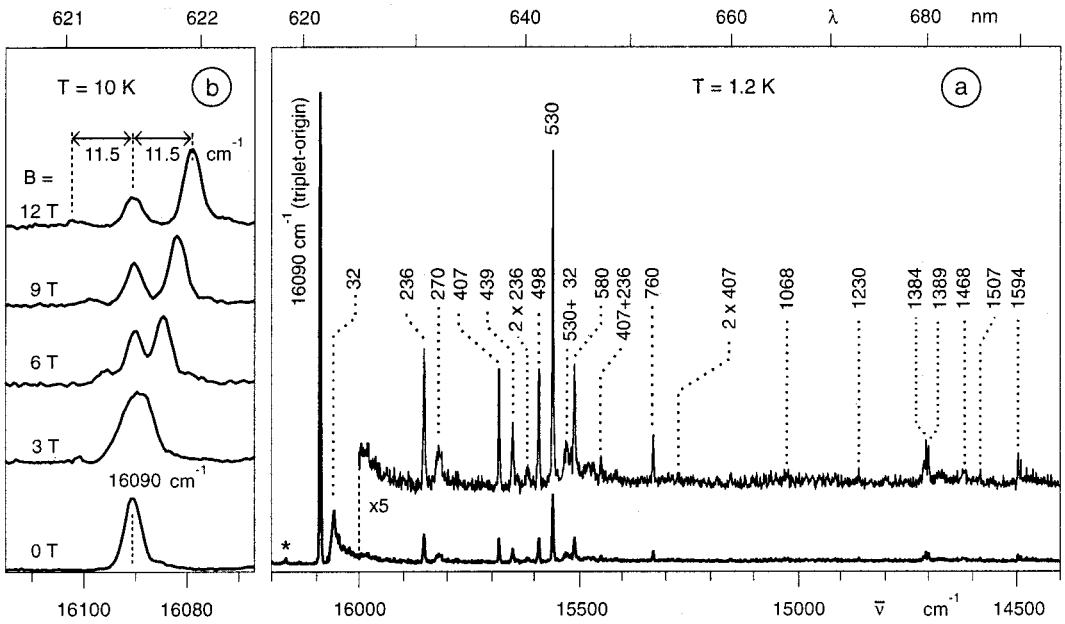

Figure 1. (a) Triplet emission spectrum of $Pd(qol)_2$ in *n*-octane (Shpol'skii matrix) at $T = 1.2$ K ($c \approx 10^{-5}$ mol/L). The compound is selectively excited at 20 617 cm^{-1} (0−0 transition of $S_0 \rightarrow {}^1$ILCT). The emission represents a spectrum of the lowest site A in the *n*-octane matrix. The asterisk indicates a residual intensity of the electronic origin of site B at 16 167 cm^{-1}. The vibrational satellites are specified relative to the electronic origin (^{3}ILCT $\rightarrow S_0$) at 16 090 cm^{-1} (site A). (b) Emission spectra in the range of the triplet origin for different magnetic fields (scale expanded, $T = 10$ K). The intensities are not comparable.

excitation at 20 617 cm^{-1} (485.04 nm) into the singlet S_1 of site A (see below) one obtains the triplet emission spectrum, which results exclusively from site A. This spectrum is reproduced in Figure 1a for $T = 1.2$ K. It shows one dominating peak at 16 090 cm^{-1} (electronic origin) and a rich vibrational satellite structure, as will be discussed in the following subsections.

The emission spectrum of site B cannot be measured separately without also observing the emission from site A, since the singlet absorption of site B overlaps with the absorption of site A. Therefore, the emission of site B is not further discussed here, but see the results presented in section 3.2.

3.1.1. Electronic Triplet Origin. The peak of highest energy at 16 090 cm^{-1} is assigned as the electronic origin (0−0 transition) corresponding to the ^{3}ILCT state of site A. It is expected that a corresponding transition would also be observed in an excitation spectrum at the same energy. However, this was not found. Obviously, the radiative transition moment between this triplet and the singlet ground state is too small to allow us to record the triplet excitation spectra. The weak transition probability is also indicated by the relatively long emission decay times (see below). Nevertheless, it is still possible to classify the peak at 16 090 cm^{-1} as the electronic origin due to the general structure of the spectrum and the good fit of the satellites to vibrational energies. (Compare the next subsection.) The zero-field splittings of the electronic origin into the three substates **I**, **II**, and **III** could not be resolved in the emission spectrum with lines of inhomogeneous line widths of ~3 cm^{-1}. Obviously, the zfs is much smaller, and indeed, this will be shown in section 3.2.

Besides the occurrence of long emission decay times, the triplet nature of this excited state is directly demonstrated by the splitting of the electronic origin into three components under application of magnet fields up to $\mathbf{B} = 12$ T (Figure 1b). The temperature for these experiments is chosen to be 10 K, since at lower temperatures, the high-energy Zeeman component would not be observable in emission due to being frozen out. The splitting is symmetric, and from a value of 11.5 cm^{-1} between two sublevels at $\mathbf{B} = 12$ T one obtains a *g* factor of 2, which corresponds to the free electron value or to the high-field limit. This result is reasonable, since the total Zeeman splitting at $\mathbf{B} = 12$ T is more than a factor of 100 larger than the observed zero-field splitting (see section 3.2).

3.1.2. Vibrational Satellites. The peaks, found in the emission spectrum of Figure 1a at lower energy than the electronic origin at 16 090 cm^{-1} (0−0 transition), reflect a number of very interesting and important properties of $Pd(qol)_2$. Generally, below about 100 cm^{-1} relative to the electronic origin, one finds lattice modes or local phonon modes, which carry information about the interaction between the chromophore and the matrix cage (e.g., the 32 cm^{-1} peak). Up to about 600 cm^{-1}, one finds metal−ligand (M−L) vibrations (e.g., 236 and 407 cm^{-1}), and at higher vibrational energies one observes internal ligand vibrations (e.g., 760, 1384, and 1594 cm^{-1}), apart from M−L progressions (e.g., 2×407 cm^{-1}) (Table 1). This general classification is consistent with assignments of the spectra of many other compounds (e.g., see refs 1−11, 30−32, 39, and 40). The vibrational satellites observed in low-temperature emission spectra correspond to vibrations of the electronic ground state and should be compared to IR and/or Raman data, which, however, are not yet available, but the observed values correspond well to those of $Pt(qol)_2$, apart from a slight high-energy shift of vibrations of the latter compound. For example, the vibrations at 236 and 407 cm^{-1} of $Pd(qol)_2$ correspond to 253 and the 413 cm^{-1} of $Pt(qol)_2$, respectively. (See Table 1 and refs 30 and 32.) A similar blue shift (high-energy shift) of vibrational energies has also been observed for $Pt(2\text{-thpy})_2$ compared to $Pd(2\text{-thpy})_2$.[40] This behavior of slightly larger force constants for Pt(II) compared to Pd(II) compounds does not seem to be unusual.[41] With respect to the present

(39) Flint, C. D.; Matthews, A. D. *J. Chem. Soc., Faraday Trans. 2* **1976**, *72*, 579.
(40) Wiedenhofer, H.; Schützenmeier, S.; von Zelewsky, A.; Yersin, H. *J. Phys. Chem.* **1995**, *99*, 13385.
(41) Nakamoto, K. *Infrared and Raman Spectra of Inorganic and Coordination Compounds*; Wiley-Interscience: New York, 1978.

Table 1. Prominent Vibrational Energies (cm^{-1}) of the Electronic Ground State (S_0) and of ^{1}ILCT of $Pd(qol)_2$ Dissolved in *n*-Octane ($T = 1.2$ K)

vibrational satellites			vibrational satellites		
$^3ILCT \rightarrow S_0$ (0−0), 16 090 cm^{-1} [a]	$S_0 \rightarrow {}^1ILCT$ (0−0), 20 617 cm^{-1} [a]	assignments and comparison to $Pt(qol)_2$	$^3ILCT \rightarrow S_0$ (0−0), 16 090 cm^{-1} [a]	$S_0 \rightarrow {}^1ILCT$ (0−0), 20 617 cm^{-1} [a]	assignments and comparison to $Pt(qol)_2$
32	32	lattice mode/31[b]	580		584[b]
55		lattice mode/53[b]	642		407 + 236
236	∼240	progression-forming mode/253[b]	760	∼770	767[b]
		distinct Pd−N component	815		2 × 407
270		277[b]	1068	∼1070	
407		progression-forming mode/413[b]	1230		1230[b]
		distinct Pd−N component	1384		1386[b]
439		446[b]	1389		1391[b]
473		2 × 236	1468		1468[b]
498	∼490	499[b]	1507		1508[b]
530		538[b]	1594	∼1580	1600[b]
562	∼560	530 + 32			

[a] Site A. [b] Vibrational energies of the electronic ground state of $Pt(qol)_2$ dissolved in *n*-octane (from ref 30).

investigation, it is important that by use of the reference peak at 16 090 cm^{-1} one can determine correct vibrational energies.

The intensity of the electronic origin is much larger than that of any vibrational satellite. This is an indication that the satellites are mainly Franck−Condon induced and that progressions may occur (compare refs 42−46). Indeed, the second members of the progressions of the 236 and 407 cm^{-1} modes are clearly observed (Figure 1a and Table 1). However, they are still very weak. From the intensity distributions of these progressions one can determine the corresponding Huang−Rhys factors S to be ≈0.1 for both vibrations. These Huang−Rhys factors correspond to the extents of the shifts of the equilibrium positions between the involved electronic states. (Compare refs 1 (p 165), 3, 30, and 43−46.) Compared to the known range of S values observed for other compounds—values up to 10 and even larger have been reported (for example, see refs 43−46)—it follows that a Huang−Rhys factor of 0.1 must be regarded as being very small. This implies very similar equilibrium positions for the electronic ground state and the triplet sublevel(s). For vibrational modes other than those at 236 and 407 cm^{-1}, we did not find any second member of a progression. Most of these other satellites observed in the emission spectrum of Figure 1a are probably also Franck−Condon induced, since the intensity at the electronic origin carries significant allowedness. In this situation, the intensities of vibronically induced satellites according to a Herzberg−Teller mechanism are usually small compared to the Franck−Condon induced ones. (Compare refs 2, 40, 42−45, and 47.) Thus, one may conclude that the Huang−Rhys factors or the shifts of the equilibrium positions along these vibrational coordinates are still smaller than those occurring for the 236 and 407 cm^{-1} modes.

The vibrational modes at 236 and 407 cm^{-1} may be characterized by analogy to those of $Pt(qol)_2$,[30,32] as largely exhibiting Pd−N and Pd−O vibrational character, respectively. Interestingly, the intensities of the corresponding satellites are much larger than found for the intensities of typical vibrational ligand modes (∼600−1700 cm^{-1}). From this behavior, it can be concluded that the spatial region of the two-ring heterocycle, which is the main origin of the high-energy ligand modes, is not so strongly involved in the process of charge reorganization. Rather, the electronic transitions occur in the spatial regions of the coordinating oxygen and nitrogen atoms. Indeed, such a specific intensity distribution is expected for ILCT transitions, in which changes of charge density occur in the region of oxygen and nitrogen. (For a more detailed discussion of this general aspect see refs 1, 30, and 47−49.) For completeness, it is mentioned that the intensity distribution of the vibrational satellites is different, for example, for typical $\pi\pi^*$ transitions, as are found in $[Rh(bpy)_3]^{3+}$, where the satellites of vibrational internal ligand character strongly dominate,[1,3] or in $[Os(bpy)_3]^{2+}$, where, due to MLCT transitions, both internal ligand and vibrational metal−ligand satellites have high intensities.[1]

Table 2. Emission Energies (0−0 Transitions), ODMR Line Positions, and Emission Lifetimes of the Triplet Sublevels of $Pd(qol)_2$ in *n*-Octane ($T = 1.4$ K) for the Two Different Sites

	zero-phonon line (cm^{-1}) (intensity (%))	$2E$ (MHz) ($\epsilon_{III} - \epsilon_I$)	$D - E$ (MHz) ($\epsilon_I - \epsilon_{II}$)	lifetimes of triplet substates (ms)		
				I	**II**	**III**
site A	16 090 (75)	2356	5241	90	0.18	0.08
site B	16 167 (25)	2329	5215	80	0.18	0.10

3.1.3. Emission Decay. After pulsed excitation into a higher lying state ($\lambda_{exc} = 337.1$ nm ≙ 29 665 cm^{-1}), one observes at $T = 1.2$ K a non-monoexponential decay. Usually, the three triplet sublevels are populated differently in the course of the intersystem crossing. Due to the fact that normally they are not thermally equilibrated[1,3,9−25,30−32,50−52] at $T = 1.2$ K, one should observe a triple-exponential decay. However, the decay curve (not reproduced) can perfectly be fitted double-exponentially with decay times of 80 ± 10 and 180 ± 10 μs. Obviously, one decay component is missing. A careful search for this component by use of the usual emission decay measurements was unsuccessful. However, as will be shown below in section 3.2 (Figure 5), a zero-field microwave recovery signal clearly reveals a third component of about 90 ms. We assign the three decay components in the following sequence: $\tau_I = 90$ ms, $\tau_{II} = 180$ μs, and $\tau_{III} = 80$ μs (Table 2).

With temperature increase the decay becomes monoexponential and reaches an average value of $\tau_{av} = 150$ μs at $T \approx 20$

(42) Hochstrasser, R. M. *Molecular Aspects of Symmetry*; W. A. Benjamin Inc.: New York, Amsterdam, 1966.
(43) Solomon, E. I. *Comments Inorg. Chem.* **1984**, *5*, 225.
(44) Denning, R. G. In *Vibronic Processes in Inorganic Chemistry*; Flint, C. D., Ed.; *Mathematical and Physical Sciences 288*; Kluwer Academic Publishers: Dordrecht, The Netherlands, 1989; p 111.
(45) Wilson, R. B.; Solomon, E. I. *J. Am. Chem. Soc.* **1980**, *102*, 4085.
(46) Yersin, H.; Otto, H.; Zink, J. I.; Gliemann, G. *J. Am. Chem. Soc.* **1980**, *102*, 951.
(47) Gastilovich, E. A. *Sov. Phys. Usp. (Engl. Transl.)* **1991**, *34*, 592.
(48) Braun, D.; Huber, P.; Wudy, J.; Schmidt, J.; Yersin, H. *J. Phys. Chem.* **1994**, *98*, 8044.
(49) Yersin, H., Humbs, W. *Inorg. Chem.* **1999**, *38*, 5820.
(50) Tinti, D. S.; El-Sayed, M. *J. Chem. Phys.* **1971**, *54*, 2529.
(51) Scott, P. L.; Jeffries, C. D. *Phys. Rev.* **1962**, *127*, 32.
(52) Donges-Becker, D.; Yersin, H.; von Zelewsky, A. *Chem. Phys. Lett.* **1995**, *235*, 490.

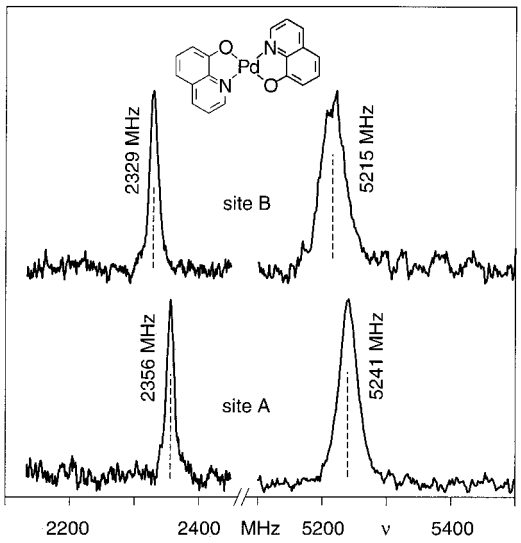

Figure 2. Zero-field ODMR spectra of $Pd(qol)_2$ in an *n*-octane Shpol'skii matrix in the excited triplet state, excitation wavelength 457.9 nm, $T = 1.4$ K. Site A: Detection wavelength 621.5 nm (16 090 cm^{-1}). Site B: Detection wavelength 618.7 nm (16 167 cm^{-1}). The intensities of the signals are normalized with respect to the maxima.

K. (Compare also ref 31.) This behavior results from strongly temperature-dependent processes of spin−lattice relaxation,[14,15,50,51] which lead to fast thermalization of the three triplet sublevels and consequently to the appearance of one averaged decay component. In general, three processes of spin−lattice relaxation have to be taken into account,[14,15,51] namely, the direct, the Orbach, and the Raman processes. A T^5-Raman process is probably the most important one, as may be concluded from detailed investigations[14] of other metal−organic Pt(II) compounds in the same matrix material. However, this subject requires further study. (Compare also ref 52.)

3.2. Triplet ODMR and PMDR Spectroscopy. Luminescence spectroscopy as is applied is not suited to resolve the zero-field splittings of the triplet, when they are smaller than about 0.5−1 cm^{-1}. However, ODMR spectroscopy can provide the corresponding information and can be used to characterize the triplet substates further. Figure 2 shows zero-field ODMR spectra for $Pd(qol)_2$ as detected at the electronic origins of the two different sites in the *n*-octane matrix. For each of the two sites A and B two zero-field ODMR transitions are observed. The resonance frequencies for these transitions are given in Figure 2 and Table 2. Conversely, the emission spectra, being related to each of the ODMR transitions, were measured also in a phosphorescence microwave double-resonance (PMDR) experiment. In the latter, one probes the spectral dependence of the microwave-induced changes in the emission intensity, keeping the microwave frequency on-resonance with one of the zero-field transitions. The PMDR spectra obtained for the two resonances at 2356 MHz (site A) and 2329 MHz (site B) as well as the normal emission spectrum are presented in Figure 3. As illustrated, one can separate the emission spectra for the two sites A and B in the matrix by use of the PMDR spectroscopy.

Recently, Glasbeek and Yersin et al.[11] reported a single zero-field ODMR signal for $Pd(2\text{-thpy})_2$ at 2886 MHz. From an analysis of the shift and the broadening of the 2886 MHz signal, observed when magnetic fields up to about 400 G were applied, it followed that the signal corresponds to a 2*E* transition. The zero-field $D \pm E$ transitions, however, remained unobserved in the ODMR experiment. The *D* value was estimated to be larger than 6600 MHz (0.22 cm^{-1}). The transition frequencies found

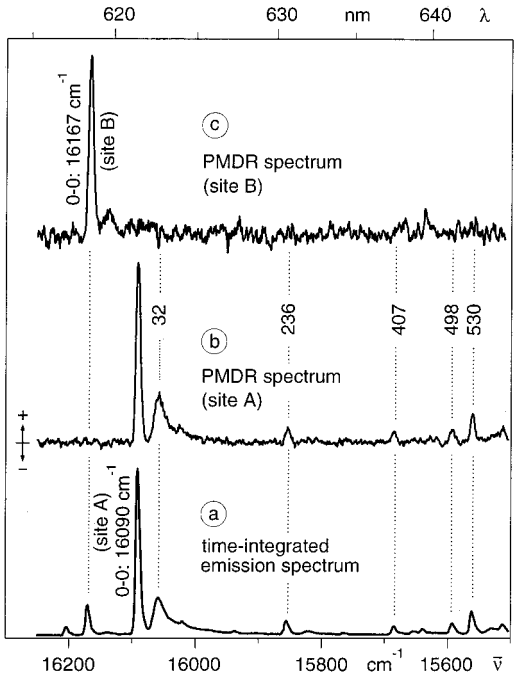

Figure 3. (a) Time-integrated emission spectrum of $Pd(qol)_2$ in *n*-octane at $T = 1.4$ K, nonselectively excited at 457.9 nm. (b) PMDR spectrum induced by microwave excitation of the 2356 MHz zero-field resonance of site A. (c) PMDR spectrum induced by microwave excitation of the 2329 MHz zero-field resonance of site B. An intensity increase (+) signifies that the emission from the short-lived sublevel **III** is increased at the expense of an emission from the long-lived sublevel **I**. For both PMDR spectra (b) and (c) the optical excitation was at 457.9 nm.

for $Pd(qol)_2$ at 2356 MHz (site A) and 2329 MHz (site B) as zero-field signals (see Figure 2) are comparable in magnitude to the value of 2886 MHz for the 2*E* transition in $Pd(2\text{-thpy})_2$. It is suggested, therefore, that the two former transitions correspond also to the 2*E* transitions of $Pd(qol)_2$. To further substantiate this interpretation, the behavior of these transitions in small magnetic fields (<400 G) was examined. With an increase of the magnetic field strength the ODMR signals shifted, broadened, and rapidly decreased in total intensity. For fields higher than about 400 G the signals became too weak to be observed. In Figure 4a, typical ODMR data for the low- and high-frequency ODMR transitions are shown for site A for different magnetic field strengths.

It has been shown elsewhere[53,54] that for an ensemble of randomly oriented triplet spins with zero-field splitting parameters, which are related by $D \geq 3E > 0$, the 2*E* and the $D + E$ transitions undergo positive frequency shifts and the $D - E$ transition undergoes a negative frequency shift (the shift for the 2*E* transition being largest), when small magnetic fields are applied (low-field limit). In addition to shifts, the magnetic field will also induce broadening effects for the ODMR transition. It was shown[53,54] that the broadening gives rise to asymmetrically shaped ODMR signals. The resonance frequencies corresponding to the maxima in the asymmetrically shaped resonances are shifted for all three transitions in a positive sense with respect to the zero-field values. As illustrated in Figure 4a, the 2356 MHz resonance shows a positive frequency shift in a magnetic field (100 MHz in a field of 200 G). This

(53) McCauley, E. M.; Lasko, C. L., Tinti, D. S. *Chem. Phys. Lett.* **1991**, *178*, 109.
(54) McCauley, E. M., Lasko, C. L., Tinti, D. S. *J. Phys. Chem.* **1992**, *96*, 1146.

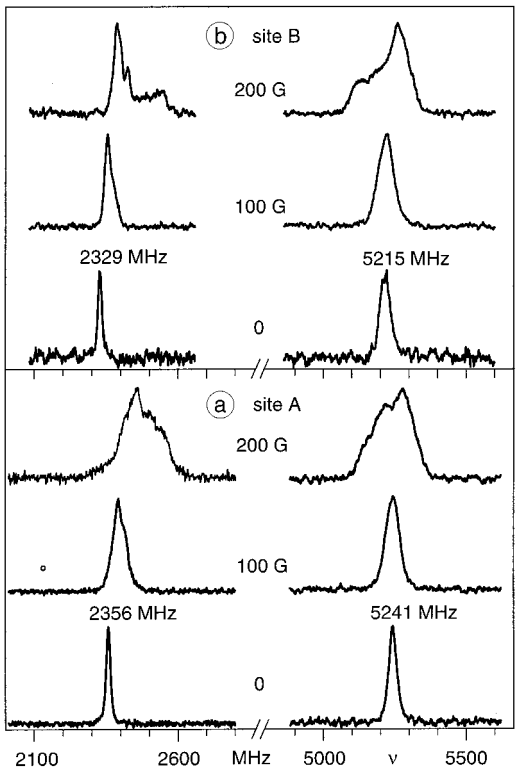

Figure 4. ODMR spectra of $Pd(qol)_2$ in various (small) external magnetic fields for the two sites A and B. Magnetic fields are given in gauss ($1\ G = 10^{-4}$ T).

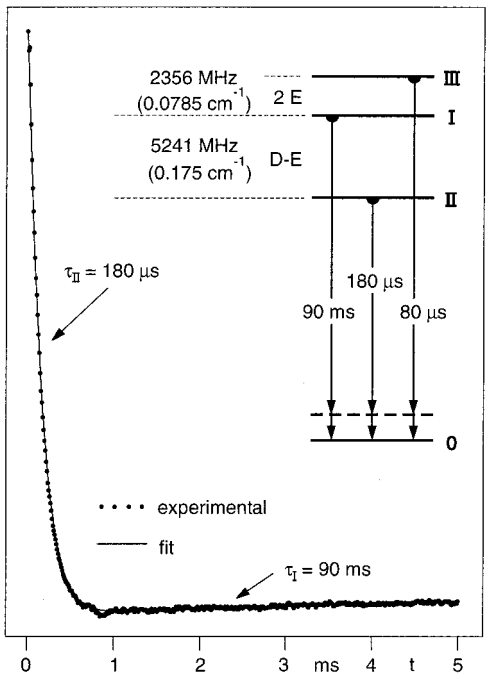

Figure 5. Zero-field microwave recovery signal for the $D - E$ transition at 5241 MHz for $Pd(qol)_2$ in a Shpol'skii matrix at 1.4 K (site A). (Intensity in linear scale) The drawn curve is a fit to $f(t) = A \exp(-t/\tau_a) + B \exp(-t/\tau_b)$ with $A = 6.3$, $B = -0.2$, $\tau_a = 180\ \mu$s, and $\tau_b = 90$ ms. The inset shows the energy level diagram for the three triplet substates and the corresponding emission decay times of site A.

frequency shift is larger than that of the 5241 MHz transition of site A, for which the maximum is shifted by only 30 MHz to higher frequency for $\mathbf{B} = 200$ G. Moreover, for the latter transition, one clearly observes a broadening that is larger on the low-frequency wing. All these features observed for the ODMR transitions of site A for $Pd(qol)_2$ in the Shpol'skii matrix are compatible with the field effects predicted in a simple perturbation approach to the aforementioned limit of $D \geq 3E > 0$. Thus, one can assign the zero-field ODMR transitions at 2356 and 5241 MHz to the $2E$ and $D - E$ triplet sublevel transitions, respectively. Consequently, one obtains for site A $D = 6419$ MHz (0.214 cm^{-1}) and $E = 1178$ MHz (0.039 cm^{-1}). Since the ODMR spectra were measured for an ensemble of randomly oriented molecules in the triplet state, further specification of the orientation of the magnetic axes within the $Pd(qol)_2$ molecule cannot be given.

Similar ODMR results were also obtained for site B. As illustrated in Figure 4b, the low-frequency transition at 2329 MHz is shifted to higher frequencies as the magnetic field strength is increased. Furthermore, the resonance has its steepest rise on the low-frequency side and a larger broadening at the high-frequency side as expected for the magnetic field effect on a $2E$ transition.[53,54] In a magnetic field, the maximum of the high-frequency zero-field signal for site B at 5215 MHz shows a positive shift, whereas the broadening at the low-frequency wing is in accordance with the behavior expected for the $D - E$ transition in the low-field limit in the case $D \geq 3E > 0$. Thus, one obtains for site B $D = 6380$ MHz (0.213 cm^{-1}) and $E = 1165$ MHz (0.0388 cm^{-1}).

For both sites, one expects that the $D + E$ transition occurs in the frequency range of 7560−7600 MHz. However, experimentally, no ODMR signal in this range could be measured. Alternatively, an attempt was made to measure the $D + E$ transition in an optically detected electron−electron double-resonance (EEDOR) experiment (e.g., compare ref 55). In the latter, the power from a second microwave source was swept, while the frequency of the first microwave source was kept at a constant value, on-resonance with the $2E$ transition. Indeed, in zero magnetic field, for each site a weak EEDOR signal could be monitored (spectra not shown), but the signal was characteristic of the $D - E$ resonance only, while the $D + E$ transition remained unobserved. The EEDOR signal is generally much weaker than the ODMR signal, since basically *changes* in ODMR intensities are measured. This may be the reason the $D + E$ EEDOR transition could not be observed.

The zero-field splitting parameters for the phosphorescent triplet state of $Pd(qol)_2$ are comparable to those for $Pd(2\text{-thpy})_2$; the latter has $D \geq 6600$ MHz and $E = 1443$ MHz.[11] On the other hand, compared to Rh(III) chelates (with typical zero-field splittings of $D \approx 3000-4000$ MHz and $E \approx 800-900$ MHz), the zero-field splitting values for the Pd(II) complexes are significantly larger. This result suggests that spin−orbit coupling—induced by metal-d and/or MLCT admixtures to the triplet wave functions—is significantly stronger for the Pd(II) compounds compared to the Rh(III) complexes. (Compare also refs 1, 3, and 4.)

Lifetimes of the sublevels of $Pd(qol)_2$ in the emissive triplet state can be determined by means of microwave recovery experiments. In these experiments, changes of phosphorescence intensity induced by applied resonant microwave pulses are measured with time. Under low-temperature conditions and no microwave application, the triplet sublevels are thermally isolated from each other (they are not in thermal equilibrium). After application of resonant pulses, the individual lifetimes of the microwave-pumped triplet sublevels are reflected in the kinetics of the recovery signal.[11,20−22] Figure 5 shows a typical

(55) Kuan, T. S.; Tinti, D. S.; El-Sayed, M. A. *Chem. Phys. Lett.* **1970**, *4*, 507.

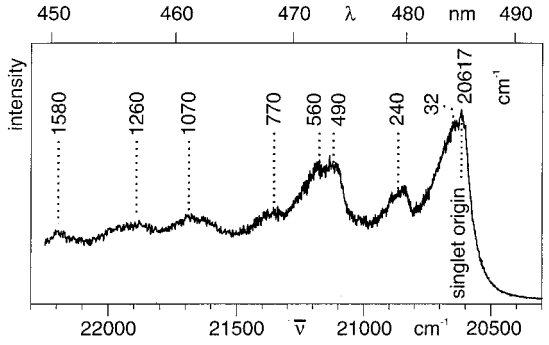

Figure 6. Singlet excitation spectrum ($S_0 \rightarrow {}^1$ILCT) of $Pd(qol)_2$ in *n*-octane at $T = 1.2$ K, detection of the emission at 16 090 cm^{-1} (electronic origin ^{3}ILCT $\rightarrow S_0$ of site A). The vibrational satellites are specified relative to the electronic origin at 20 617 cm^{-1}. The spectrum is not corrected with respect to the characteristics of the laser dyes (coumarin 47 and 102).

transient, probed for the $D - E$ transition of site A. As is obvious, the recovery signal is non-monoexponential. It can be well fitted to biexponential behavior. Labeling the triplet substates as **I**, **II**, and **III**, such that $\epsilon_{III} > \epsilon_I > \epsilon_{II} > 0$ (i.e., $2E = \epsilon_{III} - \epsilon_I$ and $D - E = \epsilon_I - \epsilon_{II}$; see also the inset of Figure 5), the sublevel lifetimes for site A are fitted to $\tau_I = 90 \pm 30$ ms and $\tau_{II} = 180 \pm 10$ μs. In particular, the decay component of $\tau_{II} = 180 \pm 10$ μs is also observed in the low-temperature phosphorescence decay (see section 3.1.3). This latter experiment provides additionally the $\tau_{III} = 80 \pm 10$ μs component. The value of τ_{III} was verified independently from the measured microwave recovery signal for the $2E$ zero-field transition. Thus, the three decay components are determined and summarized in Table 2 and Figure 5. Slightly different results are obtained for site B with $\tau_I = 80 \pm 30$ ms, $\tau_{II} = 180 \pm 10$ μs, and $\tau_{III} = 100 \pm 10$ μs.

Interestingly, these decay components allow us to understand the intensity increase of the PMDR spectrum by use of the $2E = 2356$ MHz resonance, for example, for site A (see Figure 3b). This resonance equilibrates the two states **I** and **III**. Since the emission from **I** is strongly forbidden, as is reflected in the long decay time of $\tau_I \approx 90$ ms, application of this microwave frequency opens the pathway toward the more radiative sublevel **III** and thus leads to an increase of emission intensity.

Moreover, the result that the $D + E$ zero-field ODMR transition remains unobserved may also be explained. From the time-resolved experiments it follows that this transition is the one between the triplet sublevels with the shorter lifetimes. In this respect, the situation is similar to that of $Pd(2\text{-thpy})_2$ in the phosphorescent triplet state. For $Pd(2\text{-thpy})_2$ the resonance between the sublevels with lifetimes of 134 and 235 μs remained unobserved in zero-field ODMR.[11] The two sublevels with the shorter lifetimes seem to show little population difference also for $Pd(qol)_2$, as has been shown in ref 10 for Pd(2-thpy). Therefore, detection of an ODMR transition between these sublevels will be difficult.

3.3. Site-Selective Singlet Excitation. Figure 6 shows a low-temperature excitation spectrum of $Pd(qol)_2$ doped into *n*-octane. In the same energy range one finds a broad and unstructured absorption peak at $T = 298$ K ($\bar{\nu}_{max} \approx 22\,500$ cm^{-1}, half-widths (fwhm) ≈ 2500 cm^{-1}, $\epsilon_{max} \approx 6000$ L/mol cm in DMF, spectrum not reproduced), which obviously corresponds to the same transition as is recorded in the excitation experiment. The high value of the molar absorption coefficient allows us to assign the corresponding excited state to a singlet, namely, to ^{1}ILCT. Further arguments for this classification are presented in section 4 and in refs 30−32.

The excitation spectrum is recorded by selectively detecting the triplet emission at the electronic origin of site A at 16 090 cm^{-1}. Thus, the singlet excitation represents also a site A spectrum with the electronic origin at 20 617 cm^{-1}. This energy is determined by fitting the peak with a Lorentzian line shape function. (A fit using a Gaussian line shape was not successful, as is particularly obvious from the low-energy tail of the line shape function.) The occurrence of a Lorentzian line shape for the electronic origin at 20 617 cm^{-1} indicates that the spectrum is homogeneously broadened.[56,57] Therefore, the half-width, which is determined to be $\Delta\bar{\nu} \approx 80$ cm^{-1} (fwhm), can be related in the low-temperature limit to the lifetime of this state by $\tau(^1\text{ILCT}) = (2\pi c\Delta\bar{\nu})^{-1}$, wherein c is the velocity of light measured in cm/s, if $\Delta\bar{\nu}$ is measured in cm^{-1}.[57] (This expression is determined by use of the Heisenberg uncertainty principle according to $\Delta E \cdot \tau = h \cdot \Delta\nu \cdot \tau \approx \hbar$; e.g., compare ref 56.) The resulting value of $\tau(^1\text{ILCT}) \approx 2 \times 10^{-13}$ s ($k \approx 5 \times 10^{12}$ s^{-1}) is even shorter than that found for $Pt(qol)_2$.[30] Presumably, the decay of the ^{1}ILCT state is governed not only by processes of intersystem crossing to the ^{3}ILCT state, but additionally by relaxation processes to dd* states, which are expected to lie between the ^{1}ILCT and ^{3}ILCT states, probably not far from 19 000 cm^{-1}.[32]

The structure of the excitation spectrum (Figure 6) at higher energy is assigned to result from vibrational satellites. It is possible to determine a number of vibrational energies from the energy separations of the electronic origin at 20 617 cm^{-1}. The resulting values are marked in Figure 6 and summarized in Table 1. Interestingly, one finds a relatively good agreement with the vibrational energies of the electronic ground state. This indicates similar force constants for these states. However, a more detailed interpretation along these lines does not seem to be reasonable due to the relatively large line widths of the respective peaks.

4. Orbital Assignment and Conclusion

The resolved $S_0 \rightarrow S_1$ excitation spectrum shown in Figure 6 corresponds to the characteristic but unresolved absorption band at $\bar{\nu}_{max} \approx 22\,500$ cm^{-1} (at $T = 298$ K in DMF). Equivalent absorption bands with similar shapes but slightly different values for $\bar{\nu}_{max}$ were also found for the uncoordinated quinolinol ligand as well as for $Al(qol)_3$, $Pt(qol)_2$, and qol^- compounds of other metal ions.[26,32] The transition found for the uncoordinated ligand has been assigned to an electron charge-transfer transition from the oxygen part of the molecule to the nitrogen region, or from the phenolic side to the pyridyl part of the quinolinol two-ring system.[58−61] The near correspondence of the absorption band of the uncoordinated ligand with those of the metal complexes leads to the suggestion that the same type of orbital jump occurs for all of these molecules.[26,30] Following the notation introduced by Vogler et al.,[33] we characterize this electronic transition as an intraligand charge-transfer (ILCT) transition and the corresponding singlet state as ^{1}ILCT.

An alternative assignment of the low-energy absorption band or excitation structure of $Pd(qol)_2$ is not very likely, since (i) an LMCT transition should lie at much higher energy,[26] (ii)

(56) Demtröder, W. *Laser-Spektroskopie*; Springer-Verlag: Berlin, 1991; p 42 ff.
(57) Dick, B.; Nickel, B. *Chem. Phys.* **1986**, *110*, 131.
(58) Bailey, A. S.; Williams, R. J. P.; Wright, J. D. *J. Chem. Soc.* **1965**, 2579.
(59) Goldman, M.; Wehry, E. L. *Anal. Chem.* **1970**, *42*, 1178.
(60) Burton, R. E.; Davis, W. J. *J. Chem. Soc.* **1964**, 1766.
(61) Bardez, E.; Chatelain, A.; Larrey, B.; Valeur, B. *J. Phys. Chem.* **1994**, *98*, 2357.

dd*-metal-centered transitions would be much weaker (e.g., see ref 62), and (iii) MLCT transitions which might occur in this energy range can be ruled out, since the observed absorption bands are also found in closed shell metal compounds such as $Al(qol)_3$, for which such a low-energy MLCT transition can be excluded (e.g., see ref 26).

The triplet emission having its electronic origin (0−0 transition) at 16 090 cm^{-1} (site A) is assigned to result predominantly from the same orbital character. Thus, the corresponding state is ^{3}ILCT. The information discussed in the previous sections provides strong support for this classification. In particular, the vibrational satellite structure (section 3.1.2) clearly shows that the spatial regions of the Pd−O and Pd−N vibrational modes are involved in the electronic transitions as is expected for an ILCT transition. The alternative assignment to an MLCT transition can be easily excluded due to the small zero-field splittings on the order of only 0.1 cm^{-1} (section 3.2), since for a typical ^{3}MLCT state, as occurs in $[Ru(bpy)_3]^{2+}$, one finds zfs which are orders of magnitude larger (e.g., see refs 1 and 4). Moreover, the very long emission decay time of substate **I** of $\tau_I \approx 90$ ms and the very low transition probabilities for all three triplet sublevels (not excitable) are more characteristic of a ligand-centered than of an MLCT transition. Similarly, assignments to triplets of MC (metal-centered dd*) or LMCT character can be excluded. Finally, a triplet resulting from a ligand-centered $\pi\pi^*$ transition would exhibit similarly small values of zfs and long decay times, but the intensity patterns of the vibrational satellite structures would be different. One would observe much higher vibrational satellite intensities in the range of the typical ligand modes than observed for $Pd(qol)_2$ (compare refs 1, 3, 4, and 49).

(62) Lever, A. B. P. *Inorganic Electronic Spectroscopy*, 2nd ed.; Elsevier Publishers: Amsterdam, The Netherlands, 1984; p 550.

In conclusion, the assignment of the emitting state to a ^{3}ILCT state seems to be well substantiated. Moreover, in $Pd(qol)_2$ this state contains only very small metal-d or MLCT admixtures. Nevertheless, this small metal participation seems to be manifested in the magnitude of the zero-field splitting parameter *D*, which is larger than expected for purely ligand transitions. Under the condition that singlet and triplet excited states belong to the same orbital parentage, the energy difference between the electronic origins of the ^{1}ILCT and ^{3}ILCT states is to a first approximation determined by twice the exchange interaction. The resulting value of 4527 cm^{-1} is much too small for a typical $\pi\pi^*$ transition, but fits well to a charge-transfer transition. Interestingly, corresponding values are also known for $Pt(qol)_2$ and Pt(qtl), being 3341 and 2035 cm^{-1}, respectively.[31] This behavior seems to show that the corresponding ILCT transitions are spatially increasingly extended from $Pd(qol)_2$ to $Pt(qol)_2$ and to $Pt(qtl)_2$. This property seems at least in part to be connected with an increasing (though still small) MLCT admixture to the ILCT states. Indeed, the larger metal participation in the ^{3}ILCT state of $Pt(qol)_2$ compared to $Pd(qol)_2$ is distinctly displayed, for example, in much shorter emission decay times and higher radiative rates for the transitions between ^{3}ILCT and the electronic ground state. However, the zfs is still smaller than $\approx$1 cm^{-1}, which demonstrates that even in $Pt(qol)_2$ the metal character in the ^{3}ILCT state is relatively small compared to that in compounds such as $[Ru(bpy)_3]^{2+}$ and $[Os(bpy)_3]^{2+}$ (e.g., compare refs 1, 3, and 4).

Acknowledgment. We gratefully acknowledge financial funding of the Deutsche Forschungsgemeinschaft (DFG) and the Verband der Chemischen Industrie. J.K.N. thanks Bowdoin College for sabbatical leave support and the Fulbright Foundation for a Fulbright senior scholar award.

IC991023L